Science of Sintering, **54** (2022) 39-48

https://doi.org/10.2298/SOS2201039S

UDK 522.52; 53.086

Characterization of Sedimentary Minerals from Kolubara Mining Basin, Serbia, with the Determination of Natural Radioactivity

Aleksandra Šaponjić[1], Stanislav Gyoshev[2], Zvezdana Baščarević[3], Ljiljana Janković Mandić[1], Gorica Ljubenov[4], Maja Kokunešoski[1*)]

[1]Institute of Nuclear Sciences "Vinča", National Institute of theRepublic of Serbia, University of Belgrade, Serbia

[2]Institute of Information and Communication Technologies, Bulgarian Academy of Sciences, Bulgaria

[3]Institute for Multidisciplinary Research, University of Belgrade,Serbia

[4]Faculty for Constriction Management, University Union - Nikola Tesla, Serbia

Abstract:

Diatomite (diatomaceous earth) and clay minerals deposits from the mining basin Kolubara, Serbia, are natural materials with high economic potential in many fields. As received and treated materials, diatomite and clay were characterized using X-ray diffraction, mercury intrusion porosimetry, particle size distribution, scanning electron microscopy, and Fourier-transform infrared spectroscopy. Activity concentrations for natural radionuclides 40K, ^{226}Ra and ^{232}Th and anthropogenic radionuclide ^{137}Cs in diatomite and clay were determined by gamma spectrometry with HPGe detector. For diatomite and clay, the mean activity concentrations of ^{226}Ra, ^{232}Th and 40K were found to be 9, 26 and 173 Bq kg^{-1} and 19, 26 and 470 Bq kg^{-1}, respectively. In the present study was to show that these materials are environmentally safe for further use in many fields.

***Keywords**: Diatomite;Clay;Particle size distribution; Natural radionuclides.*

1. Introduction

During coal exploitation from surface coal mine Kolubara, Serbia, a huge amount of diatomite and clay sedimentary minerals were deposited as accompanying minerals. Diatomite or diatomaceous earth is of sedimentary origin consists mainly of accumulated skeletons formed as a protective covering of the diatoms. Diatomite is typically soft, friable and fine-grained, characterized by a relatively low density, chemically inert in most liquids and gases and sparingly soluble in water. Also, this natural material has low thermal conductivity and high absorption capacity. Diatomite usually finds application as filters, heat insulators, absorbents, catalyst supports and advanced environmental applications such as membranes or chromatography columns [1-9]. This material has traditionally been used as building materials and thermal insulation [10]. Clay generally consists of a mixture of different clay minerals and associated minerals. The most abundant clays are minerals from the smectite group, with a 2:1-layer structure comprises sheets linked by weak van der Waals forces [11]. Smectite is the name used for a group of phyllosilicate mineral species, the most

*) **Corresponding author:** majako@vin.bg.ac.rs; maja.kokunesoski@gmail.com

important being montmorillonite, beidellite, nontronite, saponite and hectorite. Montmorillonite, as the most common mineral from the smectite group ((1⁄2Ca,Na)(Al,Mg,Fe)4(Si,Al)$_8$O$_{20}$(OH)4nH2O) is the main constituent of bentonite, derived by weathering of volcanic ash [12]. Clays are used in drug delivery systems, agrochemical delivery agents, and catalytic materials [13-19]. Radionuclides such as ^{40}K and radionuclides from ^{232}Th and ^{238}U series and their decay products in soils that occur in minerals are adsorbed into soil components (organic matter, carbonates, iron and manganese oxides). From an environmental point of view, processes of their transfer and bioavailability are important [20-21].

The main constituent of diatomite and clay is SiO_2, so these sediments are often used for the synthesis of SiO_2 based ceramics [22-26]. Commercially used diatomite is generally produced from natural diatomite by calcination processing at about 900^{o}C. Clay minerals can be chemically treated to activate its pore structure and/or the surface of the solid. Acid activation of clay minerals (e.g., montmorillonite, bentonite) is a common chemical modification to enhance its adsorption capacity and give it certain properties for desirable applications [7]. Adsorption is an effective method for quickly lowering the concentration of the environmental organic compound in an effluent [27].

In this study, we determined the properties of diatomite and clay before and after thermal and chemical treatments by using X-ray diffraction (XRD), particle size distribution, scanning electron microscopy (SEM), and Fourier-transforminfrared spectroscopy (FTIR). Since the starting materials are of geological origin it is to be expected that those materials possess natural radioactivity. Concentrations of activity of natural radionuclides ^{40}K, ^{226}Ra and ^{232}Th in diatomite and clay were determined by gamma spectrometry with a high-resolution hyper purity germanium detector (HP Ge) which is important for further use.

The main goal of this work were to study the feasibility of utilizing diatomaceous earth and clay by physical and chemical characterization to show that these materials are environmentally safe for further use in many fields.

2. Materials and Experimental Procedures

2.1 Chemicals and purification procedure

As-received diatomite and clay were purchased from coal mine Kolubara (Serbia). Purification procedures have been done for as-received diatomite and clay using thermal and chemical treatments (treated samples). Organic impurities from sedimentary minerals have been removed by heat treatment at 600^{o}C for 2 h in air. Thermal treatment has also been found to be effective for removing Fe to leach iron [25]. After thermal treatment, in an aqueous solution of 0.5 M HCl (p.a. 37%, BDH Prolabo) (wt% 1:10) sedimentary minerals were chemically treated by stirring for 6 h at 60^{o}C. Sediments were dried at 120^{o}C until the constant weight.

2.2 Methods

The XRD of as-received and treated samples was done at room temperature using Ultima IV Rigaku diffractometer, equipped with Cu K$\alpha_{1,2}$ radiation, with generator voltage 40.0 kV and generator current 40.0 mA. The range of 5°-60° *2θ* was used in a continuous scan mode with a scanning step size of 0.02° at scan rate of 10 °/min. An ANALYSETTE 22 Micro-Tec plus was employed to determine particle size distribution. The microstructure analysis is performed by SEM, VEGA TS 5130 MM, Tescan. The functional groups of diatomite and clay were studied by using FTIR spectroscopy. The powder samples with a small amount of KBr were pressed in a mould and introduced into a Perkin Elmer FT-IR spectrometer, Spectrum Two. The spectral data of the sample were collected between

1200and 450 cm^{-1}. The HP Ge gamma-ray spectrometry system, ORTEC-AMETEK, with 49% relative efficiency was used to determine the activity concentration of ^{226}Ra, ^{232}Th and^{40}K in the samples. Each sample was counted for 60ks, and the analysis of the obtained gamma spectra was performed with the use of the software Gamma Vision 32. The absorbed gamma-ray dose rates (D, in nGy h^{-1}) in the air at 1 m above the ground is calculated using the following equationD (nGy h^{-1}) = 0.0417 AK + 0.462 ARa+ 0.604 AThby the [21], where AK, ARa, ATh are the activity concentrations of ^{40}K, $^{22}6Ra$ and ^{232}Th, in Bq kg^{-1} respectively.

3. Results and Discussion

3.1 Properties of as-received and treated diatomite

The silica content of the diatomite powder is (in wt.%) 73.68. The other impurities present in the diatomite powder are Al_2O_3-12.28, Fe_2O_3-3.29, CaO-0.70, MgO-0.44, Na_2O-0.12, K_2O-1.01 and weight loss 8.26 [28]. Wet chemical methods determined the chemical composition of as-received diatomite.

The XRD patterns of as-received and treated diatomite are depicted in Fig. 1. The XRD analysis revealed that diatomite had a typical opal structure. The X-ray diffraction pattern of the heat-treated diatomite (Fig. 1) shows that amorphous silica transformed into quartz (PDF no. 33-1161).

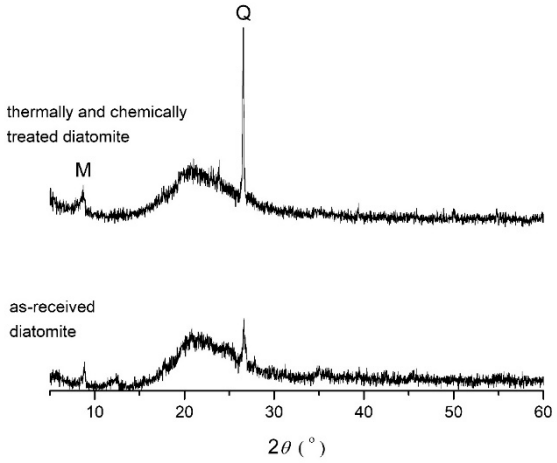

Fig. 1. XRD patterns of as-received and thermally and chemically treated diatomite.
Q PDF no.33-1161 quartz, SiO_2; M PDF no.74-2428 muscovite, $K_2(AlSi_3O_{10})(F,OH)_2$.

The XRD pattern shows the broadening of the diffraction lines in the regions around 15–25º of 2θ, associated with the present amorphous silica phase. Quartz (peak of quartz at about 26° 2θ, PDF no. 33-1161) is the major crystalline phase in the as-received diatomite and thermally and chemically treated samples [22]. Quartz is preferred over amorphous silica for many applications because of its greater chemical and thermal stability [2]. As accompanying mineral muscovite is observed (PDF no.74-2428) [22,26,28].

Scanning electron microscope images of as-received diatomite are shown in Fig. 2 and Fig. 3b. The frustules have a disk, capsule-shaped with a middle circular opening. Regularly spaced rows of fine pores run along the cylindrical walls. They possess pitted surface areas with fine pores. The frustules also appear as short tubes with rows of fine pores aligned parallel to the tube axis (centric type). A short tube end of the frustules possesses a circular hole with a protruding outer rim (Fig. 2b). According to the shape and morphology, diatoms belong to the Aulacoseira type [29].

The specimen as-received diatomite (Fig. 3a) has almost the same particle size distribution as treated diatomite. Particle size distribution was given by an average diameter value of 26 μm for both as-received and treated diatomite. All of these observations are in good agreement with results obtained by the SEM analyses (Fig. 3b). Particle size distribution and SEM image of treated diatomite samples were not provided due to similarity with as-received diatomite.

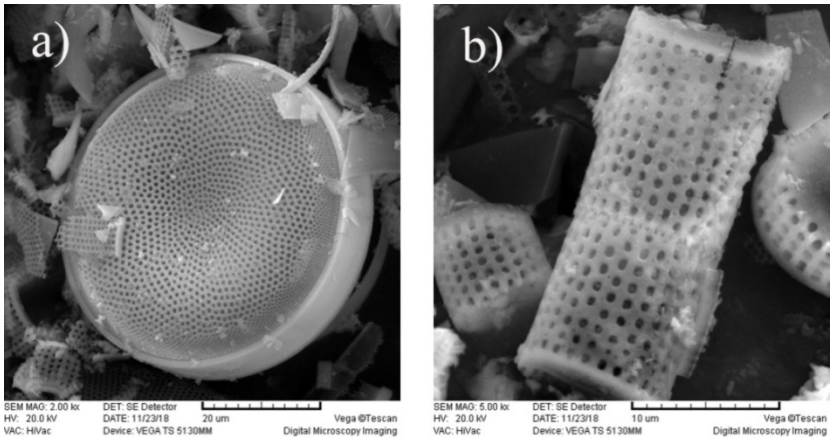

Fig. 2. SEM image of frustules of as-received diatomite: a) disks and b) capsule-shaped with a middle circular opening.

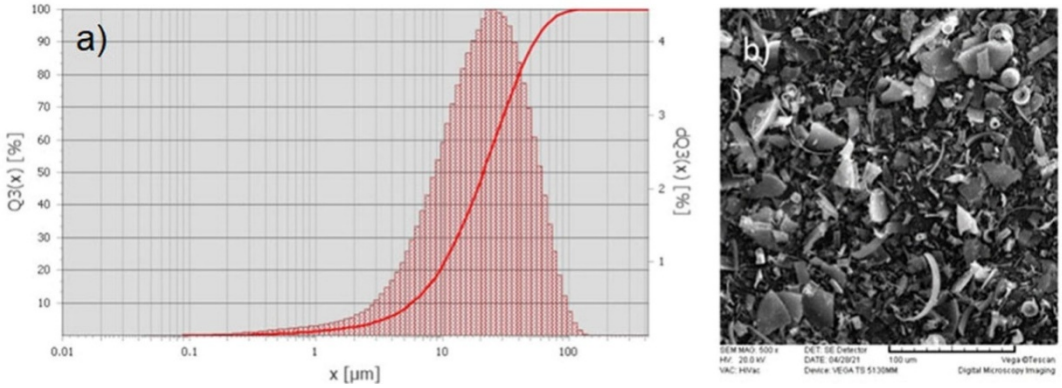

Fig. 3. As-received diatomite: a) particle size distribution curve, and b) SEM images of disks and frustules.

Fig. 4 shows FTIR as-received and treated diatomite spectrums. In the observed spectrums, the absorption bands at 1050 cm^{-1}, 795 cm^{-1} and 446 cm^{-1} are the characteristic bands for modified SiO_2 amorphous silica phase, opal. Partial arrangement of SiO_2 modification toward quartz structure (X-ray diffraction, Fig. 1.) has been presented with a weak absorption band in 693 cm^{-1}. Absorption bands at 1054 cm^{-1} and 795 cm^{-1} are assigned to Si–O–Si plane vibrations, while the band at 446 cm^{-1} refers to Si–O–Si deformation vibrations. The clay minerals in as-received diatomite indicates a weak absorption band at 916 cm^{-1} [7, 28, 30]. A combination of weak absorption bands at 533 cm^{-1} and 446 cm^{-1} could probably correspond to Si–O (bending) deformation and Al–O stretching vibrations [31]. After the chemical and thermal treatments, absorption bands at 916 cm^{-1}, 693 cm^{-1} and 533 cm^{-1} are missing.

The activity concentrations of ^{226}Ra, ^{232}Th, ^{40}K and ^{137}Cs in diatomite samples are determined by gamma-ray spectrometry. The ^{226}Ra activity concentration varied, ranging 5-12

Bq kg^{-1} with a mean of 9 Bq kg^{-1}, ^{232}Th in the range 22-33 Bq kg^{-1} with a mean of 26 Bq kg^{-1} and ^{40}K in the range 150-190 Bq kg^{-1} with a mean of173 Bq kg^{-1}. UNSCEAR reports the worldwide average activity concentration of these radionuclides as 32, 45 and 420 Bq kg^{-1}, respectively [21]. In all samples, the activity concentration ^{137}Cs was below the detection limit.

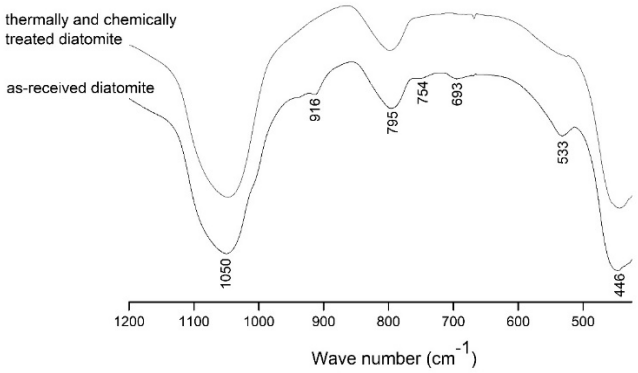

Fig. 4. FT-IR spectra of as-received and thermally and chemically treatedtreated diatomite.

The total absorbed gamma dose rate due to terrestrial radionuclides varied between 22 and 43 $nGyh^{-1}$. The mean value total absorbed gamma dose rate of 35 nGy h^{-1} was lower than the average world value (58 nGy h^{-1}).

3.2 Properties of as-received and treated clay

The chemical composition of clay obtained by the inductively coupled plasma (ICP) spectrometry (Spectro-Flame, Spectro-Analytical Instruments) shows that its main composition includes (in wt%) SiO_2-88.00, Al_2O_3-6.05, Fe_2O_3-2.06, TiO_2-0.48, CaO- 0.18, MgO-0.35, Na_2O-1.05 and K_2O-1.76 [23].

The XRD pattern of the as-received and chemically and thermally treated clay is depicted in Fig. 5. Quartz (PDF no. 33-1161) is a major phase, followed by the appearance of feldspar (PDF no. 89-8575) and smectite clays (PDF no. 229-1490) [23].

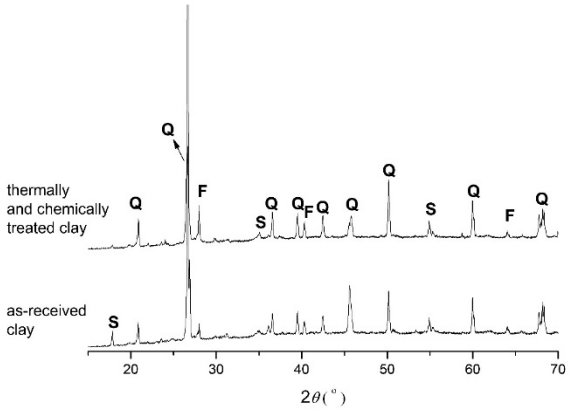

Fig. 5. XRD patterns of as-received and thermally and chemically treated clay.Q PDF no.33-1161 quartz, SiO_2; F PDF no. 89-8575 feldspar, $NaAlSi_3O_4$; S PDF no. 229-1490, smectite clays.

After thermal and chemical treatment, which removed mainly organic impurities, the clay changed its surface properties.

Particle size distribution curve and matching SEM images of as-received and treated clay are shown in Fig. 6. The treated clay (Fig. 6c) has a distinctly narrower particle size distribution compared to as-received clay (Fig. 6a). Particle size distribution was given by an average diameter value for as-received and treated clay, 22.8 μm and 52.2 μm, respectively. Even though the distribution of particle sizes for as-received clay is rather wide than treated clay, the average diameter value has increased for treated clay compared to as-received clay (Fig. 6). These observations are in good agreement with results obtained by the SEM analyses (Fig. 6b and 6d). According to the shape of curves of treated clay compared to as-received (the appearance of the shoulders on both curves), these samples have another group of smaller particles whose medium diameter is ~ 3 μm (Fig. 6a and 6c).

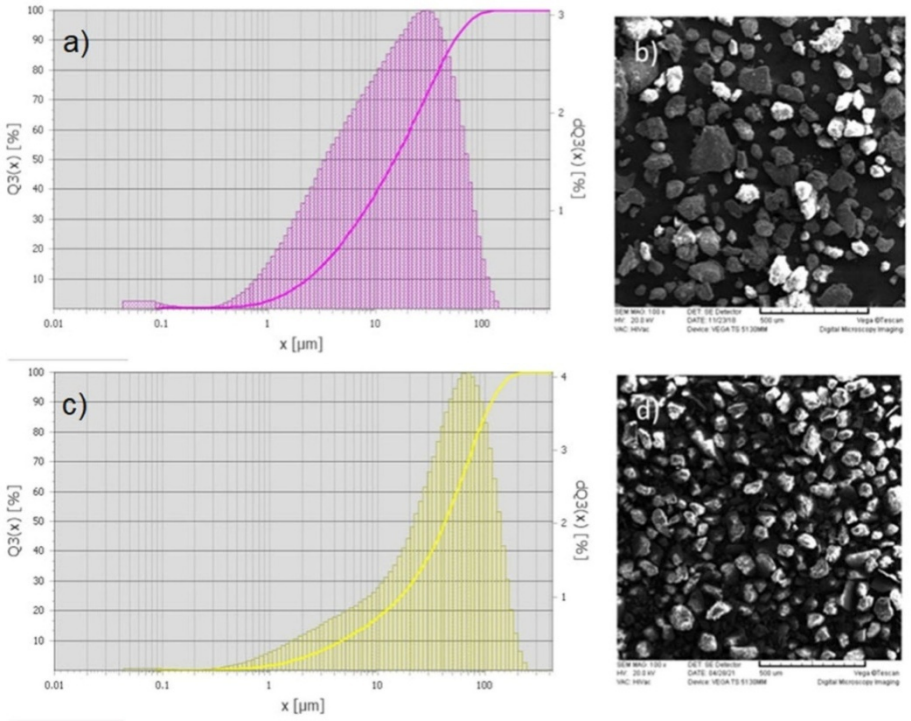

Fig. 6. Particle size distribution curve of a) as-receive and c) thermally and chemically treated clay. SEM images of b) as-received and d) treated clay.

Mostly agglomerated grains of the as-received (Fig. 7a) and treated clay (Fig. 7d) are visible in the form of lumps. Moreover, SEM images showed a layered microstructure on various magnifications (Fig. 7).

The FT-IR spectra of as-received and treated clay are displayed in Fig. 8. In the clay spectrum, characteristic wide band 1023 cm^{-1} is Si–O–Si stretching vibrations. The small wide band at 910 cm^{-1} corresponds to Al–OH–Al bending vibrations originating from OH in the di-octahedral layer [32]. A characteristic band at 795 cm^{-1} followed by the less intensive band at 777 cm^{-1}, according to the literature data, corresponds to a doublet of quartz [33,34]. The characteristic narrow band around 693 cm^{-1} is assigned to Si–O–Si bending vibrations [34]. The absorption band at 523 cm^{-1} is assigned to Si–O–Al bending vibrations stemming from oxygen in the octahedral layer. Wide band at 453 cm^{-1} originates from the Si–O–Si bending vibrations [34]. Due to thermal and chemical treatments, bands are less pronounced, while the bands at 910 cm^{-1} and 745 cm^{-1} are missing in the spectrum of the treated clay sample.

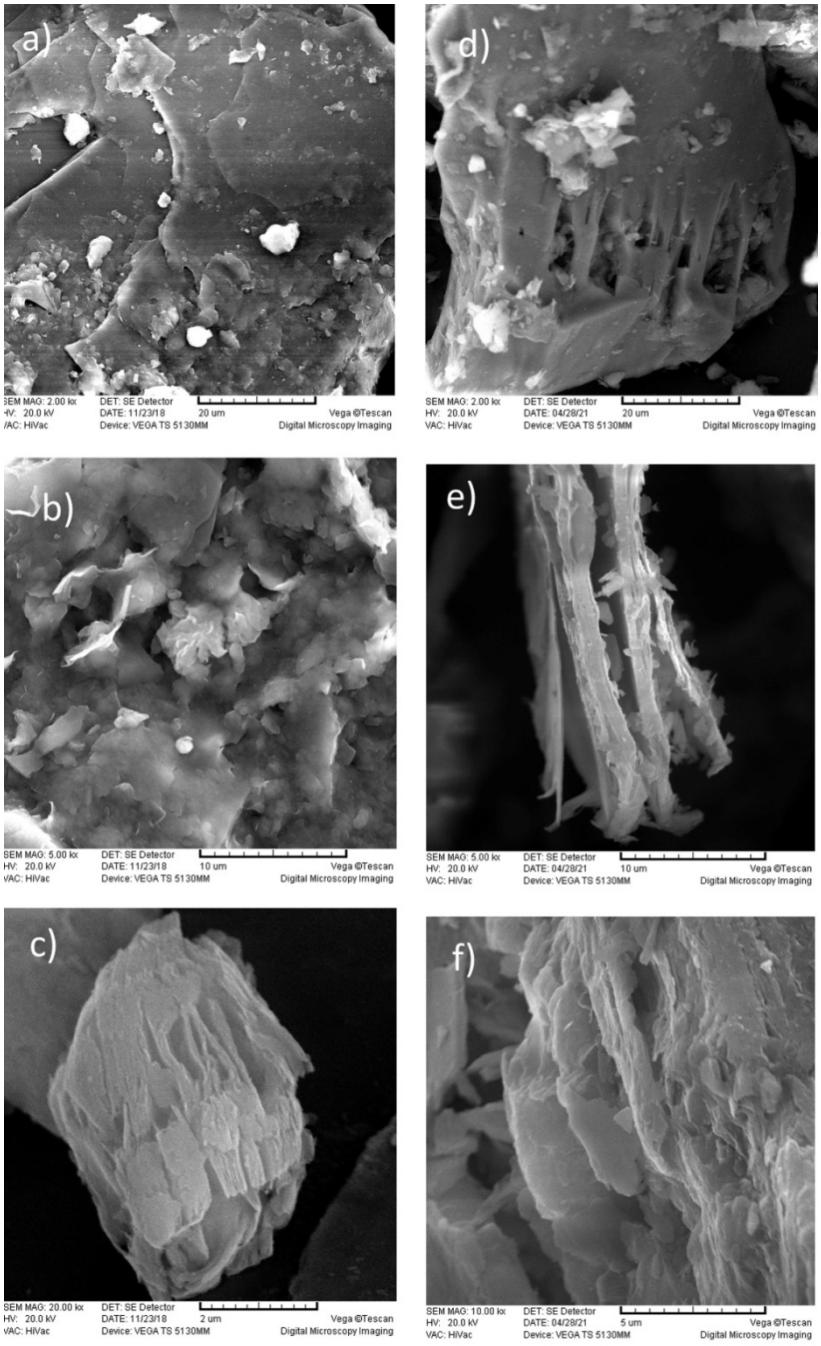

Fig. 7. SEM images (a-c) of as-received clay and (d-f) of thermally and chemically treated clay in the form of layered lumps.

The ^{226}Ra activity concentration varied in the range 14-25 Bq kg^{-1} with a mean of 19 Bq kg^{-1}, ^{232}Th in the range 23-32 Bq kg^{-1} with a mean of 26 Bq kg^{-1}and ^{40}K in the range 420-550 Bq kg^{-1} with a mean of 470 Bq kg^{-1}. UNSCEAR reports the worldwide average activity concentration of these radionuclides as 32, 45 and 420 Bq kg^{-1}, respectively [21]. In all samples, the activity concentration ^{137}Cs was below the detection limit. The total absorbed gamma dose rate due to terrestrial radionuclides varied between 39 and 54 nGyh^{-1}. The mean

value total absorbed gamma dose rate of 44 nGy h^{-1} was lower than average world value (58 nGy h^{-1}).

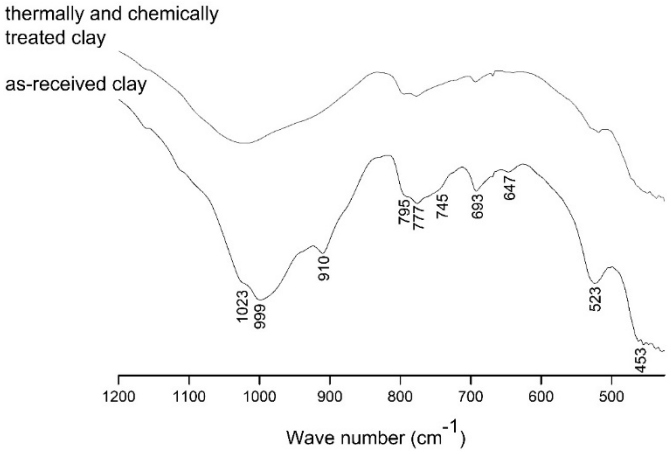

Fig. 8. FT-IR spectra of as-received and thermally and chemically treated clay.

4. Conclusion

Sedimentary mineralsfrom the mining basin Kolubara, Serbia, diatomite and clay were characterized by standard methods. After thermal and chemical treatment, the main phase in both materials was quartz, a chemically and thermally stable phase preferred for many applications. The average particle diameter value for both as-received and treated diatomite was 26 μm, while this value for as-received clay was 22.8 μm and 52.2 μm for treated clay. The scanning electron microscopy confirmed the layered microstructure of as-received and treated clay.Although the stated activity concentrations of ^{226}Ra, ^{232}Th and ^{40}K for clay were constantly above the allowed values they are however, in the recommended values, according UNSCEAR.The measured natural radioactivity of sedimentary minerals from the mining basin Kolubara, Serbia, is within the recommended safety limit. They do not pose any significant source of radiation hazard and radiological risk for further applications.

Acknowledgments

This research was funded by the Ministry of Education, Science andTechnological Development of the Republic of Serbia. Grant no. 451-03-9/2021-14/ 200017.

5. References

1. F. Akhtar, L. Andersson, S. Ogunwumi, N. Hedin, L. Bergström, J. Eur. Ceram. Soc., 34 (2014) 1643.
2. F. Akhtar, Y. Rehman, L. Bergström, Powder Technol., 201 (2010) 253.
3. C. Falamaki, M. Naimi, A. Aghaie, J. Eur. Ceram. Soc., 24 (2004) 3195.
4. D.J. Green, P. Colombo, MRS Bull., 28 (2003) 296.
5. E. Gulturk, M. Guden, J Achievements in Mat.AndManu.Eng., 46 (2011) 196.
6. M. Scheffler, P. Colombo, Cellular ceramics: Structure, manufacturing, properties and applications, Wiley-VCH, Weinheim, 2005.
7. W.T. Tsai, C.W. Lai,K.J.Hsien, J. Colloid. Interf. Sci.,297(2006)749.

8. S. Ueno, L.M. Lin, H. Nakajima, J. Am. Ceram. Soc., 91 (2008) 223.
9. P. A. M. Aguilar et al., Science of Sintering, 53(2021)137.
10. D. Wei, H.-Y. He, Sci. Sint., 51 (2019) 285.
11. J. T. Kloprogge, S. Komarneni, J. E. Amonette, Clays and Clay Minerals, 47(1999) 529.
12. G.E. Morris, M.S. Żbik, Int.J.Miner.Process.,93 (2009) 20.
13. M.J. Carrizosa, W.C. Koskinen, M.C. Hermosin, J. Cornejo, Sci. Total Environ.,247 (2000) 285.
14. M.J. Carrizosa, W.C. Koskinen, M.C. Hermosin, J. Cornejo, Appl. Clay Sci.,18 (2001)223.
15. J. Cornejo, R. Celis, L. Cox, M.C. Hermosin, Interface Sci.Technol.,1 (2004) 247.
16. J.J. Fripiat, M.I. Cruz-Cumplido, Ann. Rev. Earth Planet. Sci., 2 (1974) 39.
17. E. J. M. Hensen, B. Smit, J. Phys. Chem. B, 106 (2002) 12664.
18. T. Khalil, F. Abou El-Nour, B. El-Gammal, A.R. Boccaccini, Powder Technol.114 (2001) 106.
19. R. Suresh, S.N. Borkar, V.A. Sawant, V.S. Shende, S.K. Dimble, Int. J. Pharm. Sci.Nanotechnol.,3 (2010)901.
20. M. Tzortzis, E.Svoukis, H. Tsertos, Radiat. Protec. Dosimetry, 109 (2004) 217.
21. UNSCEAR Sources and effects of ionizing radiation, United Nations Scientific Committee on the Effects of Atomic Radiation, New York, 2010, Vol. I.
22. Lj. Kljajević, A. Šaponjić, S. Ilić, S. Nenadović, M. Kokunešoski, A. Egelja, A. Devečerski, Ceram. Int., 42 (2016) 8128
23. M. Kokunešoski, A. Šaponjić, V. Maksimović, M. Stanković, M. Pavlović, J. Pantić, J. Majstorović, Ceram. Int., 40 (2014) 14191.
24. M. Kokunešoski, A. Šaponjić, M. Stanković, J. Majstorović, A. Egelja, S. Ilić, B. Matović, Ceram. Int., 42 (2016) 6383.
25. A. Šaponjić, Dj. Šaponjić, V. Nikolić, M. Milošević, M. Marinović-Cincović, S. Gyoshev, M. Vuković, M. Kokunešoski, Sci. Sint., 49 (2017) 197.
26. A. Šaponjić, M. Stanković, J. Majstorović, A. Egelja, S. Ilić, B. Matović, M. Kokunesoski, Ceram. Int., 41(2015) 9745.
27. W.-T. Tsai, K.-J. Hsien, C.-W. Lai, Industrial and Engineering Chemistry Research 43(2004) 7513.
28. B. Matović, A. Šaponjić, A. Devečerski, M. Miljković, J. Mater. Sci., 42 (2007) 5448.
29. M. R. Crawford, Y. V. Likhoshway, R. Jahn, Diatom Research, 18 (2003) 1.
30. W. T. Tsai, C. W. Lai, K. J. Hsien, J. Colloid Interf. Sci., 297 (2006) 749.
31. V. Poharc-Logar, M. Logar, Geol. An. Balk. Poluos., 62 (1998) 233.
32. A. Obut, I. Girgin,Yerbilimleri, 25 (2002) 1.
33. G.E. Christidis, P.W. Scott, A.C. Dunham, Appl Clay Sci.,12 (1997) 329.
34. J. Madejová, M. Pentrák, H. Pálková, P. Komadel, Vibrational Spectroscopy, 49(2009) 211.

Сажетак: *Минералне наслаге, дијатомејска земља и глина из рударског базена Колубара, Србија, имају примену у многим областима као природни материјали високог економског потенцијала. Полазне и третиране сировине, дијатомејска земљана и глина, су окарактерисане рендгенскомдифракцијом, методом расподеле величине честица, скенирајућом електронском микроскопијом као и методом инфрацрвене спектроскопијеса Фоуриеровом трансформацијом. Концентрације активности природних радионуклида ^{40}K, ^{226}Ra и ^{232}Th и антропогеног радионуклида 137Cs у дијатомејској земљи и глини су одређиване гамаспектрометријски са HPGe детектором. За дијатомејску земљу утврђене су средње вредности концентрација активности ^{226}Ra, ^{232}Th и ^{40}K од 9, 26, 173 Bk kg^{-1} док су за глину ове вредности 19, 26,*

470 Bk kg^{-1}. Ова студија је показала да су ови природни материјали еколошки безбедни за даљу употребу.

***Кључне речи**:дијатомијска земља, глина,расподела величене честица, природни радионуклеиди.*